CORRUPTED REFERENCE IMAGE QUALITY ASSESSMENT

Wu Cheng and Keigo Hirakawa

Electrical and Computer Engineering, University of Dayton, 300 College Park, Dayton, OH 45469
{chengw1,khirakawa1}@udayton.edu

ABSTRACT

We propose a foundation for assessing visual quality with "corrupted reference" (CR-QA)—a new quality assessment (QA) paradigm for reasoning about human vision and image restoration problems jointly. The visual quality of a processed image signal is assessed *relative to an ideal reference image* (not provided) with the help of observed image. This is in contrast to today's QAs, which are optimized for a "post-hoc" usage (process first, assess quality second) and are unequipped to handle the assessment of the processed data relative to the ideal reference that exist only in theory and not in practice.

Index Terms— image quality assessment, image restoration

1. INTRODUCTION

Subjective quality assessment of digital images has many tangible benefits to the design of imaging systems. "Noise" and "artifacts" are best described by aspects of images that appears most unnatural to the human eye. An *objective* visual quality assessment (QA) metric aimed at unsupervised prediction of perceived quality expedites the advancement of imaging systems by replacing the subjective analysis with an automatic one. The studies resulted in three regimes of QA—full reference assessment (FR-QA) that compares the perceived similarity of a given image to the ideal reference image; reduced reference assessment (RR-QA) that retains only a few statistics of the reference image; and no reference assessment (NR-QA) which codifies the conformity to a model of a "good image."

Today's QA is optimized for a "post-hoc" usage (process first, assess quality second), such as the benchmarking illustrated in Fig. 1(a-b). This setup is particularly problematic for image restoration—the problem of recovering the latent ideal/uncorrupted signal of maximum visual quality from a given corrupted signal. The existing QAs are unequipped to handle the assessment of the processed data relative to the ideal reference that we lack access to.

This paper establishes a novel foundation for assessing visual quality with "corrupted reference" (CR-QA)—a new QA paradigm for reasoning about *human vision* and *image recovery* jointly. We prove that the visual quality of a processed image signal can be assessed relative to an *ideal* reference image (that is not provided) with the help of a *corrupted* or imperfect reference image, as illustrated in Fig. 1(c). Alternatively, CR-QA is an FR-QA computed without direct access to ideal reference. The proposed CR-QA gives rise to a new generation of visually optimal image restoration algorithms by constructively assessing the quality of reconstructed images.

2. BACKGROUND AND RELATED WORK

The performance metrics commonly used in engineering such as the mean squared error (MSE) and the related peak signal-to-noise ratio (PSNR) are known to poorly approximate the visual quality. The objective quality assessment metrics by contrast seek to incorporate low level vision and higher level human reasoning, and correspond better to the way a human observer would discriminate images. Let $\mathrm{QA}_{FR}\{x,y\}$ denote the FR-QA aimed at quantifying the perceived similarity/dissimilarity between two images, x and y, where x is the ideal reference image. The appeal of (most) FR-QA is that the maximum is attained when the two input images are identical:

$$\arg\max_y \mathrm{QA}_{FR}\{x,y\} = x.$$

Hence an optimal parameters θ in image restoration algorithms $\hat{x}(y;\theta)$ can be learned indirectly by processing representative training images with various candidate parameters, evaluating the performance of each parameter using QA as shown in Fig. 2(a), and choosing the parameter corresponding to the best quality score[1]:

$$\theta_{FR} = \arg\max_\theta \mathrm{QA}_{FR}\{x,\hat{x}(y;\theta)\}. \quad (1)$$

However, this strategy lacks signal adaptivity since θ_{FR} chosen with training data are assumed to generalize to *all* images. It is impossible to do away with training data because the ideal reference image x in $\mathrm{QA}_{FR}\{x,\hat{x}(y;\theta)\}$ is not accessible for real sensors.

The human eye discriminates image quality without access to an ideal reference. Towards the goal of giving computers similar abilities, no reference quality assessment—or NR-QA, denoted as $\mathrm{QA}_{NR}\{y\}$—replaced the ideal reference with a mathematical/ statistical model representative of a "good image." Parameters in restoration algorithms are learned by processing the given input image with various candidate parameters, evaluating the restoration outputs for each parameter using QA as shown in Fig. 2(b), and choosing the parameter corresponding to the best quality score [2, 3, 4]:

$$\theta_{NR} = \arg\max_\theta \mathrm{QA}_{NR}\{\hat{x}(y;\theta)\}.$$

However, since the goal of the image restoration is to recover the uncorrupted image, appropriate metrics are the ones that naturally gravitate towards the ideal solution x. By this, NR-QA is a poor match because x does not maximize NR-QA in all cases:

$$\arg\max_y \mathrm{QA}_{NR}\{y\} \neq x.$$

3. CORRUPTED REFERENCE QUALITY ASSESSMENT

Ideal reference in most sensing modalities exists in theory and not in practice. Hence the desired attributes of QA for this setting are:

(A) the metric describes perceptual similarity of the processed image to the ideal reference.

(B) the metric attains a maximum with the ideal reference.

(C) the metric is computed without access to the ideal reference.

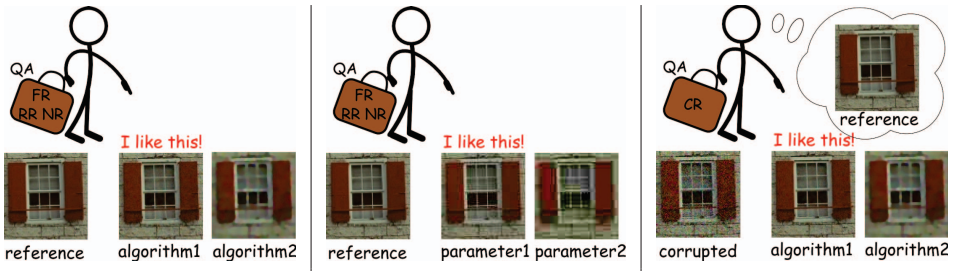

(a) algorithm evaluation (b) parameter selection (c) image restoration

Fig. 1. Applications of image quality assessment (QA). (a) QA benchmarks denoising algorithms based on the output image quality. (b) QA compares artifacts to determine the bit rate of lossy compression acceptable to a human observer. (c) Proposed technique assesses quality of images produced by restoration methods ***relative to an ideal reference image*** (not provided).

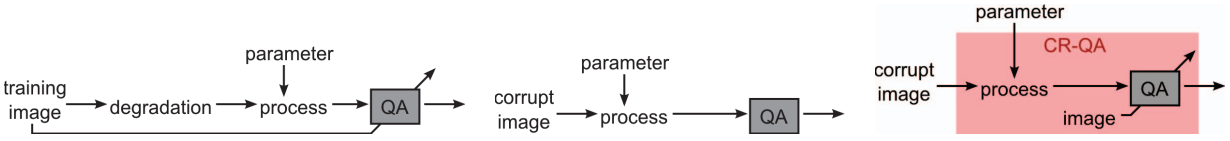

(a) FR/RR-QA (b) NR-QA (c) CR-QA (proposed)

Fig. 2. Approaches to choosing visually optimal parameters in image restoration algorithms. (a) FR/RR-QA requires training data. (b) NR-QA lacks correspondence to ideal reference image. (c) A schematic *functionally equivalent* to the corrupted reference quality assessment (CR-QA). In practice, CR-QA is computed using an alternative form because the ideal reference is not accessible.

The previous section established that existing FR/RR/NR-QAs do not accomplish these. Therefore, a quality metric satisfying all principles above is ***an entirely new category of QA*** that suits the needs of contemporary sensing applications better.

Fig. 2(c) is an example of a quality assessment strategy that satisfies the conditions (A)-(C) above. The external inputs to the system in the shaded box are the corrupted image and the processing parameter θ, but the ideal reference image used in the FR-QA is assumed to be internally available (see Section 3.1). A system that is *functionally equivalent* to the shaded box in Fig. 2(c) will be referred to as corrupted reference quality assessment—or CR-QA, denoted as

$$\mathrm{QA}_{CR}\{\hat{x}(\cdot)|y\} \qquad \text{or} \qquad \mathrm{QA}_{CR}\{\hat{x}(\cdot;\theta)|y\}.$$

Comparing schematics in Fig. 2 reveals main features of CR-QA. Unlike the modular design shown in Fig. 2(a-b), CR-QA treats both processing and QA as its internal components (hence it is specific to the image processing tasks). The output from CR-QA should match the output from Fig. 2(a) exactly when using training data:

$$\mathrm{QA}_{FR}\{x, \hat{x}(y)\} = \mathrm{QA}_{CR}\{\hat{x}(\cdot)|y\}.$$

However, Fig. 2(c) shares more in common with Fig. 2(b). In fact, one may understand CR-QA as a way to transform FR-QA into NR-QA (but without the disadvantages of NR-QA).

The structure in Fig. 2(c) have appeared previously in [5, 6] to predict the structural similarity index (SSIM) score [7] of a linear image denoising operator (which is the trivial case of (3) below). Reduced reference data can also be encoded as a side information, which is recovered later to execute RR-QA [8, 9]. However, this technique is limited to the case when the user has control over the image degradation process (e.g. compression/half-toning/watermarking).

The feasibility of CR-QA based on Fig. 2(c) depends on whether the ideal reference in FR-QA can be bypassed. Consider Stein's unbiased estimate of risk (SURE) defined by the relation [10]:

$$\underbrace{\mathbb{E}\|x-\hat{x}(y)\|^2}_{\mathrm{MSE}\{x,\hat{x}(y)\}} = \underbrace{\mathbb{E}\{\|y\|^2 + \|\hat{x}(y)\|^2 - 2y\hat{x}(y) + 2\sigma_n^2\hat{x}'(y)\} - \sigma_n^2}_{\mathrm{MSE}_{CR}\{\hat{x}(\cdot)|y\}},$$

where $\hat{x}'(y) = \sum_{i=1}^{N} \frac{\partial \hat{x}_i(y)}{\partial y_i}$ is the derivative (divergence if multivariate) and we assumed degradation $y|x \sim \mathcal{N}(x, \sigma_n^2)$. The left side of the equation is the MSE of $\hat{x}$ relative to x. The right side is a *computable* equivalent statement—it depends on y and $\hat{x}(y)$ but not x (not provided). Indeed, SURE is a type of CR-QA. Following SURE as an example, we develop CR-QA versions of SSIM [7] and visual information fidelity (VIF) [11], two well known FR-QAs. Due to page limit, we concentrate on denoising the additive white Gaussian noise ($y|x \sim \mathcal{N}(x, \sigma_n^2)$) only. However, CR-QA can be developed for other types of restoration problems and other FR-QA metrics (more discussions in Section 4).

3.1. Example #1: CR-SSIM

Denoting by $\hat{x}(\cdot)$ the estimator of ideal reference image, let SSIM assess the similarity between x and $\hat{x}(y)$ in Fig. 2(c), as follows[7]:

$$\mathrm{SSIM}\{x, \hat{x}(y)\} := \frac{(2\mu_x\mu_{\hat{x}} + c_1)(2\sigma_{x\hat{x}} + c_2)}{(\mu_x^2 + \mu_{\hat{x}}^2 + c_1)(\sigma_x^2 + \sigma_{\hat{x}}^2 + c_2)}, \qquad (2)$$

where c_1 and c_2 are constants. SSIM is not directly computable without x because it is a FR-QA, and a functionally equivalent system must be found. Most of the key statistics of SSIM can be computed by the conventional means (via the moment matching):

$$\mu_x = \mathbb{E}x = \mathbb{E}y \approx \frac{1}{N}\sum_{i=1}^{N} y_i, \qquad \mu_{\hat{x}} = \mathbb{E}\hat{x}(y) \approx \frac{1}{N}\sum_{i=1}^{N} \hat{x}_i(y)$$

$$\sigma_x^2 = \sigma_y^2 - \sigma_n^2 \approx \frac{1}{N-1}\sum_{i=1}^{N}(y_i - \mu_y)^2 - \sigma_n^2$$

$$\sigma_{\hat{x}}^2 = \mathbb{E}(\hat{x}(y) - \mu_{\hat{x}})^2 \approx \frac{1}{N-1}\sum_{i=1}^{N}(\hat{x}_i(y) - \mu_{\hat{x}})^2.$$

Finally, drawing from Stein's lemma, $\sigma_{x\hat{x}}$ takes the form [12, 10]:

$$\sigma_{x\hat{x}} = \sigma_{y\hat{x}} - \sigma_n^2\mathbb{E}\hat{x}'(y) \approx \frac{1}{N}\sum_{i=1}^{N}\Big[(y_i - \mu_y)(\hat{x}_i(y) - \mu_{\hat{x}}) - \sigma_n^2\hat{x}_i'(y)\Big],$$

(a) ideal ref. x (b) corrupted ref. y (c) denoised $\hat{x}(y)$ (d) $\mathrm{SSIM}\{x, \hat{x}(y)\}$ (e) $\mathrm{SSIM}_{CR}\{y|\hat{x}(\cdot)\}$

Fig. 3. Quality of denoised image (c) is assessed with respect to the ideal reference (a). Although CR-QA in (e) is computed without (a), it matches the full-reference result of FR-QA in (d) almost exactly. In (d-e), dark pixels=bad quality; bright pixels=good quality.

where, $\hat{x}_i'(\cdot)$ denotes the derivative (or divergence if multivariate) of the function $\hat{x}(\cdot)$. Hence following is functionally equivalent to (2):

$$\mathrm{SSIM}_{CR}\{y|\hat{x}(\cdot)\} := \frac{(2\mu_y\mu_{\hat{x}}+c_1)(2\sigma_{y\hat{x}}-2\sigma_n^2\mathbb{E}\hat{x}'(y)+c_2)}{(\mu_y^2+\mu_{\hat{x}}^2+c_1)(\sigma_y^2-\sigma_n^2+\sigma_{\hat{x}}^2+c_2)}. \quad (3)$$

Since y and $\hat{x}(y)$ are both observed, SSIM_{CR} is fully computable while maintaining functional equivalence to Fig. 2(c)—Fig. 3 illustrates that SSIM and SSIM_{CR} are nearly identical. This may be viewed as an improvement on [13, 14, 15] which reduced (but not eliminated) the dependence on the ideal image in SSIM assessment.

CR-QA is impractical unless the derivative $\hat{x}'(\cdot)$ is computable for all arbitrary high-dimensional functions. Let $\boldsymbol{y}, \hat{\boldsymbol{x}} \in \mathbb{R}^N$ be the vectorized version of y and $\hat{x}$, respectively. Then we have [16]

$$\begin{aligned}\mathbb{E}\hat{x}'(y;\theta) &= \lim_{\epsilon\to 0}\mathbb{E}\frac{\boldsymbol{w}^T(\hat{\boldsymbol{x}}(\boldsymbol{y}+\epsilon\boldsymbol{w};\theta)-\hat{\boldsymbol{x}}(\boldsymbol{y};\theta))}{\epsilon} \\ &\approx \frac{1}{N\epsilon}\boldsymbol{w}^T\Big(\hat{\boldsymbol{x}}(\boldsymbol{y}+\epsilon\boldsymbol{w};\theta)-\hat{\boldsymbol{x}}(\boldsymbol{y};\theta)\Big)\end{aligned} \quad (4)$$

where $\boldsymbol{w} \in \mathbb{R}^N$ and $w_i \overset{i.i.d.}{\sim} \mathcal{N}(0,1)$ is independent of $\boldsymbol{y}$. Equation (4) enables the computation of $\hat{x}'(\cdot)$ via the Monte-Carlo simulation of $\boldsymbol{w}$ for an arbitrarily complicated form of $\hat{x}(\cdot)$.

3.2. Example #2: CR-VIF

Let $X^j, \hat{X}_i^j(y), Y^j$ be wavelet coefficients of $x, \hat{x}(y), y$ in the jth subband, respectively. VIF models human vision as additive noise:

$$\boldsymbol{E}_i^j|\boldsymbol{X}_i^j \sim \mathcal{N}(\boldsymbol{X}_i^j, \boldsymbol{\Sigma}_V), \qquad \boldsymbol{F}_i^j|\hat{\boldsymbol{X}}_i^j(y) \sim \mathcal{N}(\hat{\boldsymbol{X}}_i^j(y), \boldsymbol{\Sigma}_V),$$

where $\boldsymbol{X}_i^j, \hat{\boldsymbol{X}}_i^j \in \mathbb{R}^M$ are nonoverlapping local neighborhoods of X^j and $\hat{X}^j$ indexed by location i, respectively. VIF assesses mutual information between X and E (and X and F) as follows:

$$\mathrm{VIF}\{x, \hat{x}(y)\} := \frac{\sum_{j,i}\log_2\left(\frac{|\operatorname{cov}(\boldsymbol{F}_i^j)|\cdot|\operatorname{cov}(\boldsymbol{X}_i^j)|}{|\operatorname{cov}(\boldsymbol{G}_i^j)|}\right)}{\sum_{j,i}\log_2\left(\frac{|\operatorname{cov}(\boldsymbol{X}_i^j)+\boldsymbol{\Sigma}_V|}{|\boldsymbol{\Sigma}_V|}\right)}, \quad (5)$$

where $\boldsymbol{G}_i^{jT} = [\boldsymbol{F}_i^{jT}, \boldsymbol{X}_i^{jT}(y)]$ and $|\cdot|$ denotes determinant. When ideal reference x is not accessible, moment matching yields

$$\operatorname{cov}(\boldsymbol{F}_i^j) = \operatorname{cov}(\hat{\boldsymbol{X}}_i^j(y)) + \boldsymbol{\Sigma}_V \approx \frac{1}{N}\sum_{i'}\hat{\boldsymbol{X}}_{i+i'}^j(y)\hat{\boldsymbol{X}}_{i+i'}^{jT}(y) + \boldsymbol{\Sigma}_V$$

$$\operatorname{cov}(\boldsymbol{X}_i^j) = \operatorname{cov}(\boldsymbol{Y}_i^j) - \boldsymbol{\Sigma}_N \approx \frac{1}{N}\sum_{i'}\boldsymbol{Y}_{i+i'}^j\boldsymbol{Y}_{i+i'}^{jT} - \boldsymbol{\Sigma}_N$$

$$\operatorname{cov}(\boldsymbol{G}_i^j) = \begin{bmatrix}\operatorname{cov}(\hat{\boldsymbol{X}}_i^j)+\boldsymbol{\Sigma}_V & \operatorname{cov}(\hat{\boldsymbol{X}}_i^j(y), \boldsymbol{X}_i^j) \\ \operatorname{cov}(\boldsymbol{X}_i^j, \hat{\boldsymbol{X}}_i^j(y)) & \operatorname{cov}(\boldsymbol{X}_i^j),\end{bmatrix}$$

where we assumed $\mu_X = \mu_Y = \mu_F = \mu_{\hat{X}} = 0$ and $\boldsymbol{\Sigma}_N$ is the noise covariance in the transform domain. By Stein,

$$\operatorname{cov}(\boldsymbol{X}_i^j, \hat{\boldsymbol{X}}_i^j(y)) = \operatorname{cov}(\boldsymbol{Y}_i^j, \hat{\boldsymbol{X}}_i^j(y)) - \sigma_n^2\mathbb{E}\hat{\boldsymbol{X}}'^j_i(y),$$

where $\hat{\boldsymbol{X}}'^j_i(\cdot)$ is Jacobian matrix of the multivariate function $\hat{\boldsymbol{X}}_i^j(\cdot)$. Thus, the following is functionally equivalent to (5):

$$\mathrm{VIF}_{CR}\{y|\hat{x}(\cdot)\} := \frac{\sum_{j,i}\log_2\left(\frac{|\operatorname{cov}(\hat{\boldsymbol{X}}_i^j(y))+\boldsymbol{\Sigma}_V|\cdot|\operatorname{cov}(\boldsymbol{Y}_i^j)-\boldsymbol{\Sigma}_N|}{|\boldsymbol{\Sigma}_G|}\right)}{\sum_{j,i}\log_2\left(\frac{|\operatorname{cov}(\boldsymbol{Y}_i^j)+\boldsymbol{\Sigma}_V-\boldsymbol{\Sigma}_N|}{|\boldsymbol{\Sigma}_V|}\right)}$$

$$\boldsymbol{\Sigma}_G = \operatorname{cov}\left(\begin{bmatrix}\hat{\boldsymbol{X}}_i^j \\ \boldsymbol{Y}_i^j\end{bmatrix}\right) + \begin{bmatrix}\boldsymbol{\Sigma}_V & -\sigma_n^2\mathbb{E}\hat{\boldsymbol{X}}'^j_i(y)^T \\ -\sigma_n^2\mathbb{E}\hat{\boldsymbol{X}}'^j_i(y) & -\boldsymbol{\Sigma}_N\end{bmatrix}, \quad (6)$$

where the Jacobian $\hat{\boldsymbol{X}}'^j_i(\cdot)$ is computed via (4).

3.3. Application of CR-QA

Denote $\hat{x}(y;\theta)$ the restoration method of corrupted image y with parameter θ. The optimal threshold parameter θ_{CR} can be retrieved by evaluating the performance of each parameter θ by $\mathrm{QA}_{CR}\{\hat{x}(\cdot;\theta)y|\}$ and simply choosing the one with best score:

$$\theta_{CR} = \arg\max_{\theta}\mathrm{QA}_{CR}\{\hat{x}(\cdot;\theta)|y\}. \quad (7)$$

In theory, this optimal value is identical to θ_{FR} in (1) since $\mathrm{QA}_{CR}\{\hat{x}(\cdot;\theta)|y\} = \mathrm{QA}_{FR}\{x, \hat{x}(y;\theta)\}$. Due to page limit, we show examples of θ_{CR} in image denoising context only (see Section 4 also). SSIM_{CR} and VIF_{CR} were used to find optimal wavelet soft threshold value [10]. As confirmed by Fig. 4 and Table 1, the selections of θ_{FR} and θ_{CR} are very close. Hence $\hat{x}(y;\theta_{CR})$ yields FR-QA optimal solution for the parametric estimator $\hat{x}$.

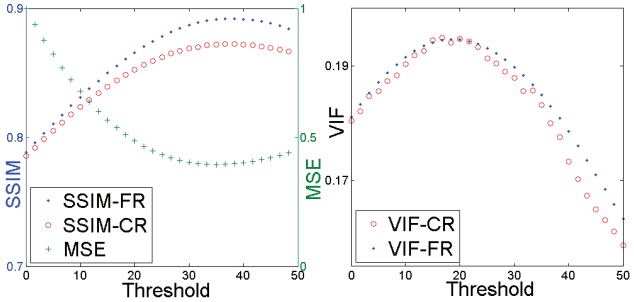

(a) SSIM vs. SSIM_{CR} (b) VIF vs. VIF_{CR}

Fig. 4. Comparisons of $\mathrm{QA}_{FR}\{x, \hat{x}(y;\theta)\}$ and $\mathrm{QA}_{CR}\{\hat{x}(\cdot;\theta)|y\}$. ($\hat{x}(y;\theta)$ is wavelet soft-thresholding with threshold θ)

Table 1. Denoising performance ($\sigma_N = 30$), averaged over 10 images[17].

QA types	$\mathbb{E}(\theta_{FR} - \theta_{CR})^2$	$\mathbb{E}(\mathrm{QA}_{FR}\{x, \hat{x}(y;\theta_{FR})\} - \mathrm{QA}_{FR}\{x, \hat{x}(y;\theta_{CR})\})^2$
MSE	21.20	5.53
SSIM	24.19	2.58e-3
VIF	35.2	2.73e-7

4. DISCUSSIONS

Previous section established that a CR-QA system functionally equivalent to Fig. 2(c) can be derived in the additive white Gaussian noise scenario. Thanks to (4), the CR-QA would predict FR-QA performance for *any* estimator $\hat{x}(\cdot)$ (not just wavelet soft thresholding). CR-QA is extendable to image restoration problems besides denoising by drawing parallels to MSE_{CR} for blur/Poisson/quantization corruptions [18, 19] (as already demonstrated in Section 3). CR-QA is extendable to FR-QA metrics besides SSIM and VIF when Stein-type equivalences are applicable.

CR-QA is not without limitations. Since the expectation operator in $QA_{FR}\{\cdot\}$ and $QA_{CR}\{\cdot\}$ are approximated by an ensemble averaging, we cannot say with absolute certainty whether the small discrepancies in Fig. 4 are due to implementation errors in FR-QA or CR-QA. In practice, *local* expectation operators in SSIM and VIF are less approximable than the global one in MSE. In addition, predictions of SSIM and VIF with SSIM_{CR} and VIF_{CR} are not *unbiased* (unlike SURE). Finally, CR-QA design assumes that the likelihood function $p(y|x)$ is known precisely. Fortunately, many high quality noise/blur parameter estimation techniques are available.

5. REFERENCES

[1] Z. Wang and A.C. Bovik, "Mean squared error: love it or leave it? a new look at signal fidelity measures," *Signal Processing Magazine, IEEE*, vol. 26, no. 1, pp. 98–117, 2009.

[2] X. Zhu and P. Milanfar, "Automatic parameter selection for denoising algorithms using a no-reference measure of image content," *Image Processing, IEEE Transactions on*, vol. 19, no. 12, pp. 3116–3132, 2010.

[3] E. Cohen and Y. Yitzhaky, "No-reference assessment of blur and noise impacts on image quality," *statistics*, vol. 12, pp. 14, 2009.

[4] D. Shaked and I. Tastl, "Sharpness measure: Towards automatic image enhancement," in *Image Processing, 2005. ICIP 2005. IEEE International Conference on*. IEEE, 2004, vol. 1, pp. I–937.

[5] S.S. Channappayya, A.C. Bovik, C. Caramanis, and R.W. Heath, "Design of linear equalizers optimized for the structural similarity index," *Image Processing, IEEE Transactions on*, vol. 17, no. 6, pp. 857–872, 2008.

[6] S.S. Channappayya, A.C. Bovik, C. Caramanis, and RW Heath, "Ssim-optimal linear image restoration," in *Acoustics, Speech and Signal Processing, 2008. ICASSP 2008. IEEE International Conference on*. IEEE, 2008, pp. 765–768.

[7] Z. Wang, A.C. Bovik, H.R. Sheikh, and E.P. Simoncelli, "Image quality assessment: From error visibility to structural similarity," *Image Processing, IEEE Transactions on*, vol. 13, no. 4, pp. 600–612, 2004.

[8] Z. Wang, G. Wu, H.R. Sheikh, E.P. Simoncelli, E.H. Yang, and A.C. Bovik, "Quality-aware images," *Image Processing, IEEE Transactions on*, vol. 15, no. 6, pp. 1680–1689, 2006.

[9] B. Hiremath, Q. Li, and Z. Wang, "Quality-aware video," in *Image Processing, 2007. ICIP 2007. IEEE International Conference on*. IEEE, 2007, vol. 3, pp. III–469.

[10] D. L. Donoho and I. M. Johnstone, "Adapting to unknown smoothness via wavelet shrinkage," *Journal of the American Statistical Association*, vol. 90, no. 432, pp. 1200–1224, 1995.

[11] H.R. Sheikh, Z. Wang, A.C. Bovik, and LK Cormack, "Image and video quality assessment research at live," `http://live.ece.utexas.edu/research/quality/`, 2003.

[12] C. Stein, "Estimation of the mean of a multivariate normal distribution," *The Annals of Statistics*, vol. 9, pp. 1135–1151, 1981.

[13] A. Albonico, G. Valenzise, M. Naccari, M. Tagliasacchi, and S. Tubaro, "A reduced-reference video structural similarity metric based on no-reference estimation of channel-induced distortion," in *Acoustics, Speech and Signal Processing, 2009. ICASSP 2009. IEEE International Conference on*. IEEE, 2009, pp. 1857–1860.

[14] Q. Li and Z. Wang, "Reduced-reference image quality assessment using divisive normalization-based image representation," *Selected Topics in Signal Processing, IEEE Journal of*, vol. 3, no. 2, pp. 202–211, 2009.

[15] A. Rehman and Z. Wang, "Reduced-reference ssim estimation," in *Image Processing (ICIP), 2010 17th IEEE International Conference on*. IEEE, 2010, pp. 289–292.

[16] S. Ramani, T. Blu, and M. Unser, "Monte-carlo sure: A black-box optimization of regularization parameters for general denoising algorithms," *Image Processing, IEEE Transactions on*, vol. 17, no. 9, pp. 1540–1554, 2008.

[17] H.R. Sheikh, Z. Wang, L. Cormack, and A.C. Bovik, "Live image quality assessment database release 2," `http://live.ece.utexas.edu/research/quality`.

[18] K. Hirakawa, F. Baqai, and P.J. Wolfe, "Wavelet-based poisson rate estimation using the skellam distribution," in *Proc. SPIE, Electronic Imaging*, 2009, vol. 7246.

[19] M. Raphan and E.P. Simoncelli, "Least squares estimation without priors or supervision," *Neural Computation*, 2010.